

## Electrical characteristics of InP with Mg-concentration gradients

M. Benzaquen and B. Belache

*Rutherford Physics Building, McGill University, 3600 University Street, Montreal, Quebec, Canada H3A 2T8*

D. Walsh

*Department of Mechanical Engineering, University of Victoria, P.O. Box 3055, Victoria, British Columbia, Canada V8W 3P6*

(Received 17 May 1990; revised manuscript received 25 March 1991)

Different InP (*p*-type) epilayers grown by metalorganic chemical vapor deposition, with one-dimensional Mg-concentration gradients perpendicular to the growth plane, have been used to study the validity of an electrical-transport model that takes this type of nonuniformity into account, and includes both the scattering mechanisms present in semiconductors and interband transitions. Secondary-ion-mass-spectroscopy measurements have been performed to determine the Mg-concentration profiles of the samples, which were required for the computation of the theoretical mobilities and free-hole concentrations. Temperature-dependent Hall-effect measurements in the range of 4.2–300 K provided the corresponding experimental quantities, which were found in good agreement with theory over a wide temperature range.

Nonuniform dopant distributions can have a considerable influence on the electrical characteristics of epitaxial semiconducting layers. The effects induced by nonuniformities can be misleading for the interpretation of electrical transport results, and their understanding is important for characterization purposes. In a review paper, Wolfe and Stillman<sup>1</sup> quoted the equations describing the Hall transport properties of nonuniform semiconductors. Subashiev and Poltinnikov,<sup>2</sup> and then Hlasnik<sup>3</sup> considered the case of extrinsic semiconductors with mobility and free-carrier concentration gradients parallel to the magnetic field and perpendicular to the electric field. This case is of interest for the understanding of the lateral electrical properties of multilayered or dopant modulated structures.

In this paper, we report on the electrical characteristics of Mg-doped InP (*p*-type) epilayers, as determined by temperature-dependent Hall transport measurements. Secondary-ion-mass-spectroscopy (SIMS) measurements are also presented, and reveal a nonuniform distribution of the Mg concentration as a function of depth in the epilayers, with Mg diffusion into the substrates. An electrical transport model which takes one-dimensional gradients (perpendicular to the surface of the epilayers) of the acceptor concentration into account is used for the analysis of the Hall data.

Mg-doped epilayers of InP were grown by low-pressure metalorganic chemical vapor deposition, on (100)-oriented Fe-doped (semi-insulating) substrates.<sup>4</sup> The *p*-dopant source was bis(methylcyclopentadienyl) magnesium (MCp<sub>2</sub>Mg). The SIMS data were collected with a Cameca IMS4f ion microprobe. Cs<sup>+</sup> primary-ion bombardment was used with detection of <sup>157</sup>CsMg<sup>+</sup>. Hall measurements were performed with a data-acquisition system<sup>5</sup> with samples shaped to a standard bridge configuration. Additional details pertaining to the experiment are provided in a previous paper.

The valence-band structure of InP consists of a light-hole (LH) band and a heavy-hole (HH) band with their

degenerated maxima at the middle of the first Brillouin zone.<sup>7</sup> Many electrical transport models were developed<sup>7–9</sup> to study extended-state conduction in uniform *p*-type III-V compounds. We use a model based on the relaxation times of Bir, Normantas, and Pikus<sup>9</sup> which has already been described.<sup>6</sup> With the assumption that the bands are parabolic and isotropic, the drift mobility for band *i* is

$$\mu = \frac{q}{m_i} \frac{\int_0^\infty \tau_{ii} P^i E^{3/2} \exp(-E/k_B T) dE}{\int_0^\infty E^{3/2} \exp(-E/k_B T) dE}, \quad (1)$$

where

$$P^i = \frac{1 + \gamma_{ij}^2 \tau_{jj} / \tau_{ij}}{1 - \tau_{11} \tau_{22} / \tau_{12} \tau_{21}} \quad (2)$$

and

$$\gamma_{ij} = \sqrt{m_i / m_j}. \quad (3)$$

*q* is the electronic charge, *m<sub>i</sub>* and *m<sub>j</sub>* are, respectively, the effective masses of band *i* and *j*.  $\tau_{ii}$  and  $\tau_{jj}$  are, respectively, the total intraband relaxation times for band *i* and *j*.  $\tau_{ij}$  and  $\tau_{ji}$  are the total interband relaxation times, corresponding, respectively, to transitions from band *i* to band *j*, and from band *j* to band *i*.

The total drift mobility is

$$\mu_T = \frac{p_{LH} \mu_{LH} + p_{HH} \mu_{HH}}{p_{LH} + p_{HH}}. \quad (4)$$

The subscripts LH and HH denote, respectively, the light and heavy holes. With nondegenerate statistics,<sup>10</sup> the total hole concentration is

$$p_T = 1/2 [ -(N_D + N_V) + \sqrt{(N_D + N_V)^2 + 4N_V(N_A + N_D)} ], \quad (5)$$

*N<sub>A</sub>* and *N<sub>D</sub>* are, respectively, the acceptor and donor

concentrations and

$$N_V = 2(2\pi m^* K_B T / h^2)^{3/2} \beta \exp(-E_A / k_B T), \quad (6)$$

where  $E_A$  is the acceptor binding energy and  $\beta = \frac{1}{4}$  the corresponding degeneracy factor.  $m^*$  is the density of states effective mass.

Both  $\mu_T$  [Eq. (4)] and  $p_T$  [Eq. (5)] are experimentally accessible quantities. They are functions of  $N_A$ ,  $N_D$ , and  $E_A$ . As  $E_A$  can be determined from freeze-out statistics,<sup>6</sup>  $N_A$  and  $N_D$  are left as the only adjustable parameters of the model as they allow the computation of  $p_T$  and  $\mu_T$  with Eqs. (1)–(6).<sup>6</sup>

Hlasnik,<sup>3</sup> on the basis of a previous work by Subashiev and Poltinnikov,<sup>2</sup> derived the mobility  $\mu$  resulting, in a Hall bridge, from mobility and concentration gradients perpendicular to the surface of the sample:

$$\mu = \frac{\int_0^t p_T(z) \mu_T^2(z) dz}{\int_0^t p_T(z) \mu_T(z) dz}. \quad (7)$$

$p_T(z)$  and  $\mu_T(z)$  are, respectively, the total free-hole concentration and the mobility at a depth  $z$ . The corresponding total free-hole concentration is

$$p = \frac{1}{t} \frac{\left( \int_0^t p_T(z) \mu_T(z) dz \right)^2}{\int_0^t p_T(z) \mu_T^2(z) dz}. \quad (8)$$

In Eqs. (7) and (8), the Hall factor  $r_H$  has been assumed to be equal to 1. The computation of  $\mu$  and  $p$  requires the mobility  $\mu_T(z)$  [Eq. (4)] and the total free-hole concentration  $p_T(z)$  [Eq. (5)] at any depth  $z$  in the sample. We have shown above that those two quantities only depend on  $E_A$ ,  $N_A$ , and  $N_D$ . Although  $E_A(z)$  varies with  $N_A(z)$  and the compensation,<sup>11</sup> it is relatively constant at the low doping levels that we will be considering,<sup>6</sup> and can be extracted, as an average, from freeze-out statistics.  $N_A(z)$  and  $N_D(z)$  allow the calculation of  $\mu_T(z)$  and  $p_T(z)$ .  $\mu$  and  $p$ , which are experimentally accessible, then follow from Eqs. (7) and (8).

Figure 1 shows the SIMS profile of the Mg concentra-

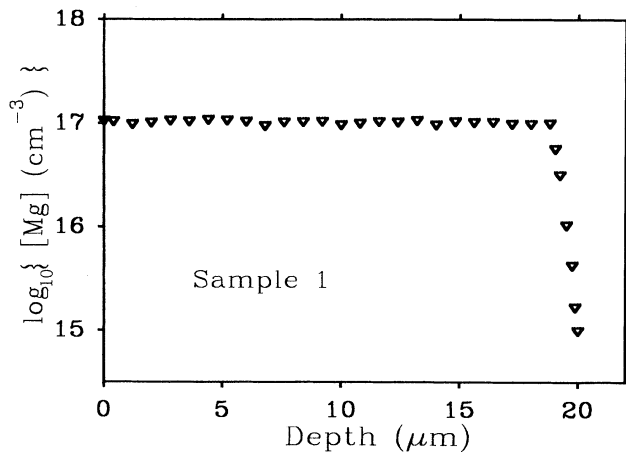


FIG. 1. SIMS Mg concentration profile of sample 1. The thickness of the conducting layer of this sample is 20  $\mu\text{m}$ .

tion ( $[\text{Mg}]$ ) of sample 1. This sample is an Fe-doped substrate, initially semi-insulating, on top of which a Mg-doped epilayer was grown and then removed by chemical etching. Consequently, the SIMS profile of Fig. 1 shows the  $[\text{Mg}]$  as a function of depth that has resulted from the diffusion of the dopant from the epilayer into the substrate during the growth process. The  $[\text{Mg}]$  is constant at a  $10^{17}\text{-cm}^{-3}$  level and extends 20  $\mu\text{m}$  into the substrate.

Figure 2 displays the SIMS profiles of the  $[\text{Mg}]$  of samples 2 and 3, which are InP epilayers grown on Fe-doped substrates. Both samples show a sharp peak of  $[\text{Mg}]$  at the interface with the substrate, which is at a depth  $z_{12} = 1.27 \mu\text{m}$  for sample 2 and at  $z_{13} = 1 \mu\text{m}$  for sample 3. An exponential increase of  $[\text{Mg}]$  from the surface of the epilayers to the onset of the spikes is observed for both samples. Sample 2, which is the most likely doped, shows very weak Mg diffusion into the substrate. Sample 3, on the contrary, has developed a  $[\text{Mg}]$  plateau in the substrate, due to diffusion, which extends to a depth  $t_3 = 1.54 \mu\text{m}$ .

The study of the diffusion mechanisms that have led to the  $[\text{Mg}]$  distribution of Figs. 1 and 2 is not required for the present work. Some results on that matter have been published,<sup>12</sup> and others are in preparation.<sup>13</sup>

Sample 1 was found to be conducting and  $p$ -type by Hall-effect measurements. The variation with temperature ( $T$ ) of its total free-hole concentration is shown in Fig. 3. The acceptor binding energy  $E_{AS}$  of this substrate is quoted in Table I. It has been extracted from freeze-out statistics<sup>6</sup> and is in good agreement with the value expected for a shallow acceptor in InP.<sup>6</sup> With  $E_{AS}$ , Eq. (5)

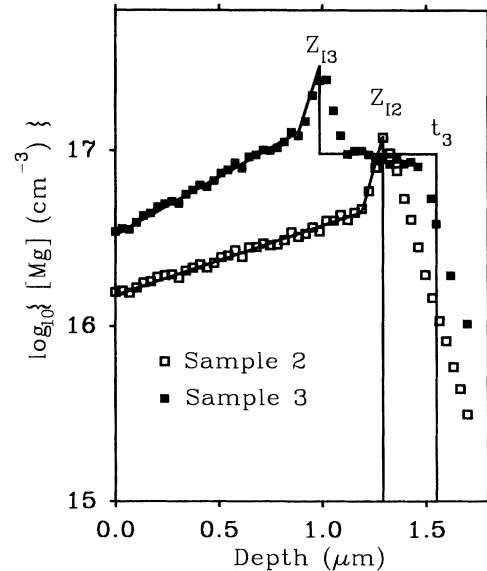


FIG. 2. SIMS  $[\text{Mg}]$  profiles of samples 2 and 3. For sample 2, the epilayer-substrate interface is at a depth  $z = z_{12} = 1.27 \mu\text{m}$ , and no significant  $[\text{Mg}]$  diffusion has occurred into the substrate. For sample 3, the epilayer-substrate interface is at  $z = z_{13} = 1 \mu\text{m}$ , and  $z = t_3$  is the depth at which  $[\text{Mg}]$  diffusion into the substrate has ended. The continuous lines are the profiles that have been assumed for the computation of the Hall parameters.

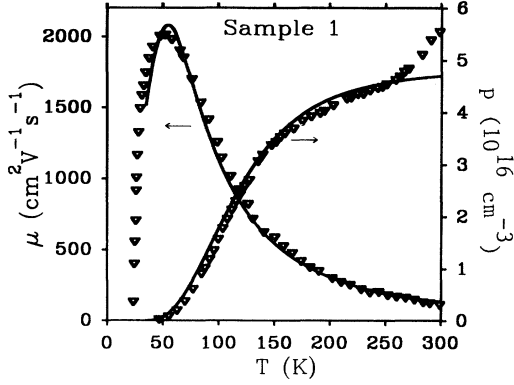


FIG. 3. Temperature dependence of the mobility and the free-hole concentration of sample 1. The continuous lines have been generated with the parameters quoted in Table I. Free-hole excitation to the valence band is observed about 280 K.

is a function of only  $N_A$  and  $N_D$ . Sample 1 is uniform, and Eq. (5) was fitted to the free-hole concentration  $p_{TS}$  of Fig. 3 with  $N_A$  and  $N_D$  as adjustable parameters. The numerical technique gave  $N_{AS} = 5.2 \times 10^{16} \text{ cm}^{-3}$  and  $N_{DS} = 3.0 \times 10^{15} \text{ cm}^{-3}$ . The corresponding continuous line of Fig. 3 was generated with those values, and provided excellent agreement with experiment in the range of 30–280 K.

Figure 3 also shows the mobility  $\mu_{TS}$  of sample 1 as a function of  $T$ . With the values of  $E_{AS}$ ,  $N_{AS}$ , and  $N_{DS}$  previously determined, Eq. (4) has been used to calculate the corresponding continuous line of Fig. 4, with excellent agreement with experiment between 30 and 280 K.  $\mu_{TS}$  could not be computed below 30 K due to too low values of  $p_{TS}$ . At 300 K, theory is 20% above experiment. The depressed room-temperature mobility of this sample can be linked to the high-temperature increase of  $p_{TS}$  observed in Fig. 3. A similar behavior has been reported for  $n$ -type InP (Ref. 14) and GaAs (Ref. 15) samples, and has been attributed to deep energy levels. The initial presence of Fe in the substrate, which is known to be a deep acceptor in InP, could support such an interpretation. The good agreement obtained between theory and experiment suggests that  $r_H$  is close to one in this case, and confirms previous observations on lightly doped  $p$ -type InP samples.<sup>6</sup> The value  $N_A = 10^{17} \text{ cm}^{-3}$ , obtained by SIMS (Fig. 1) for the [Mg] of sample 1 is different from the Hall result ( $N_{AS} = 5.2 \times 10^{16} \text{ cm}^{-3}$ ). This discrepancy suggests that the Mg atoms are not all electrically active. The electrical activity of Mg in InP is defined as

TABLE I. Results of the electrical transport analysis.  $C$  is the electrical activity of Mg in the sample.

Sample	$C$	$N_D$ ( $\text{cm}^{-3}$ )	$E_A$ (meV)
1	0.52	$3.0 \times 10^{15}$	38.3
2	0.34	$4.4 \times 10^{15}$	40.9
3	0.45	$1.3 \times 10^{16}$	37.9

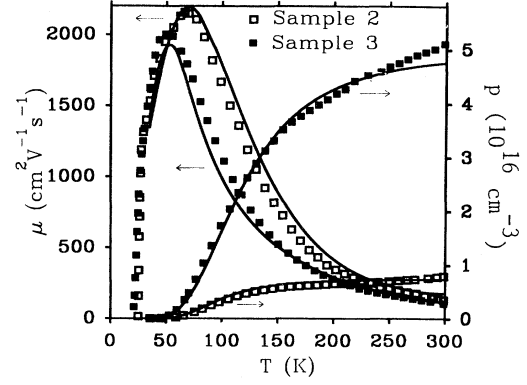


FIG. 4. Temperature dependence of the mobility and the free-hole concentration of samples 2 and 3. The continuous lines correspond to the fits of the Hall transport model for nonuniform samples to the data.

$$C = N_{AA} / [\text{Mg}], \quad (9)$$

where  $N_{AA}$  is the concentration of electrically active Mg atoms. With the above results, we find  $C = 0.52$  for sample 1.

Figure 4 displays the free-hole concentration  $p(T)$  and the corresponding mobility  $\mu(T)$  for samples 2 and 3. We denote  $f(z)$  the [Mg] distribution as a function of the depth  $z$ . In order to apply Eqs. (7) and (8) to the Hall data of Fig. 4, several assumptions are required.

(1) We have shown that the Mg atoms of the substrate are not fully electrically active. It is reasonable to assume the same for the Mg atoms of the epilayers. We then write

$$N_{AE}(z) = Cf(z), \quad (10)$$

where  $N_{AE}(z)$  is the concentration of the electrically active Mg atoms in the epilayer.  $C$  is the corresponding electrical activity.

(2) The residual donor concentrations in the epilayers ( $N_{DE}$ ) are assumed to be uniform.

The continuous line of Fig. 2 (sample 2) represents the analytical expression of  $f(z)$  that has been assumed for the epilayer of sample 2. It was obtained by fitting two exponential functions to the corresponding experimental [Mg]( $z$ ). In this case, as Mg diffusion into the substrate is very weak (Fig. 2), its effects on the electrical transport properties of the sample have been neglected. With conditions (1) and (2), Eqs. (7) and (8) are, for sample 2, functions of  $C$ ,  $N_{DE}$ , and  $E_A$ , and  $f(z)$ . An average binding energy  $E_A$  has extracted freeze-out statistics and is displayed in Table I. This leaves  $C$  and  $N_{DE}$  as the only adjustable parameters of the model. The continuous lines of Fig. 4 correspond to theory and were generated with the values of  $N_{DE}$  and  $C$  reported in Table I. The quality of the fits suggests that the model used for the analysis is satisfactory for sample 2, where a  $z$  variation of [Mg] of one order of magnitude has been observed (Fig. 2).

Sample 3, in Fig. 2, shows a significant amount of Mg diffusion into the semi-insulating substrate. In this case,  $z = z_{13}$  is the depth at the epilayer-substrate interface, and

$z=t_3$  the depth at which diffusion has ended (Fig. 2). A plateau of [Mg],  $0.3 \mu\text{m}$  wide ( $z_{13} < z < t_3$ ), is present in the substrate. We have shown, with sample 1, that this [Mg] plateau alters the electrical properties of the corresponding layer of the substrate from semi-insulating to conducting. In the epilayer of sample 3 ( $0 < z < z_{13}$ ), two exponential functions have been fitted to the corresponding [Mg] SIMS profile. They correspond to the continuous line of Fig. 2 (sample 3), and provided, as for sample 2, an analytical expression for [Mg]( $z$ ). We assume for the conducting layer of the substrate ( $z_{13} < z < t_3$ ) the same [Mg] profile as sample 1 (Fig. 1), which corresponds to the horizontal line segment of Fig. 2 (sample 3). An average  $E_A$  has been determined from the freeze-out statistics of sample 3 and is reported in Table I.  $N_{AS}$  and  $N_{DS}$  are known characteristics of the substrate, and allow, with  $E_A$ , the computation of  $\mu_{TS}(T)$  and  $p_{TS}(T)$  with the procedure described above: as for sample 2,  $C$  and  $N_{DE}$  are the only adjustable parameters in Eqs. (7) and (8). The fitting procedure provided the values reported in Table I. In Fig. 4,  $p(T)$  (sample 3, continuous line) was generated with those values in the range of 30–300 K. The corresponding  $\mu(T)$  is displayed in the same figure (sample 3, continuous line). Good agreement is found between theory and experiment. Sample 3 shows free-carrier excitation to the valence bands above 250 K, with a depressed mobility at  $T=300$  K (Fig. 4). Similar effects were observed for samples 1 and 2. The values of  $C$  quoted in Table I show that the electrical activity of

the Mg atoms of the epilayers increases with the doping level. Table I also shows that the residual donor concentration is low in the substrate. It is larger in the epilayers and increases with the doping level.<sup>6</sup> The average binding energies quoted in Table I are reasonably close to each other, as expected for lightly doped material. An interesting feature of samples 2 and 3 is the fact that despite their very different free-carrier concentrations (Fig. 4), they have similar mobilities. Samples 1 and 3 have similar electrical properties (Figs. 3 and 4) despite different [Mg] profiles (Figs. 1 and 2).

A Hall transport model, which takes into account one-dimensional gradients of the mobility and the free-carrier concentration of  $p$ -type semiconductors, has been presented. With this model we have shown that different doping profiles can yield similar electrical characteristics. We have also shown that samples with different free-carrier concentrations can give similar mobilities. The nonuniformity of the samples is responsible for those effects, which are predictable if the impurity distributions are known. The model presented can consequently be used to calculate the lateral electrical transport properties resulting from one-dimensional impurity distributions.

The authors wish to thank Dr. C. Blaauw and Dr. R. A. Bruce, from Bell-Northern Research (Ottawa) for the growth of the samples and the SIMS measurements, respectively.

<sup>1</sup>C. M. Wolfe and G. E. Stillman, in *Semiconductors and Semimetals*, edited by R. K. Willardson and A. C. Beer (Academic, New York, 1975), Vol. 10.

<sup>2</sup>V. K. Subashiev and A. S. Poltinnikov, *Fiz. Tverd. Tela (Leningrad)* **2**, 1169 (1960) [*Sov. Phys. Solid State* **2**, 1059 (1960)].

<sup>3</sup>L. Hlasnik, *Solid-State Electron.* **8**, 461 (1965).

<sup>4</sup>N. Puetz, G. Hillier, and A. J. SpringThorpe, *J. Electron. Mater.* **17**, 381 (1988).

<sup>5</sup>P. Weissfloch, M. Benzaquen, and D. Walsh, *Rev. Sci. Instrum.* **58**, 1749 (1987).

<sup>6</sup>M. Benzaquen, B. Belache, C. Blaauw, and R. A. Bruce, *J. Appl. Phys.* **68**, 1694 (1990).

<sup>7</sup>J. D. Wiley, in *Semiconductors and Semimetals* (Ref. 1), Vol. 10.

<sup>8</sup>K. Takeda, N. Matsumoto, A. Taguchi, H. Taki, E. Ohta, and

M. Sakata, *Phys. Rev. B* **32**, 1101 (1985).

<sup>9</sup>G. Bir, E. Normantas, and G. Pikus, *Fiz. Tverd. Tela (Leningrad)* **4**, 1180 (1962) [*Sov. Phys. Solid State* **4**, 867 (1962)].

<sup>10</sup>J. S. Blakemore, *Semiconductor Statistics* (Pergamon, Oxford, 1962), p. 134.

<sup>11</sup>M. Benzaquen, B. Belache, and C. Blaauw, *Phys. Rev. B* **41**, 12 582 (1990).

<sup>12</sup>E. Veuhoff, H. Baumeister, R. Treichler, and O. Brandt, *Appl. Phys. Lett.* **55**, 1017 (1989).

<sup>13</sup>C. Blaauw, B. Emmerstorfer, R. A. Bruce, and M. Benzaquen (unpublished).

<sup>14</sup>M. Benzaquen, M. Beaudoin, and D. Walsh, *Phys. Rev. B* **38**, 7824 (1988).

<sup>15</sup>M. Benzaquen, D. Walsh, R. Benzaquen, and A. Kunysz, *J. Appl. Phys.* **65**, 4874 (1989).